Lasers in Medical Science (2019) 34:1763–1779
https://doi.org/10.1007/s10103-019-02770-z

ORIGINAL ARTICLE

Laser asymmetric ablation method to improve corneal shape

José Alberto Rodríguez Agudo[1] · Jinyoung Park[1,2] · Jina Park[2] · Seongsu Lee[3] · Kisung Park[2]

Received: 11 November 2018 / Accepted: 6 March 2019 / Published online: 22 March 2019

Abstract

This study aims to assess whether central-symmetric corneal thickness reduces off-centered corneal shift caused by intraocular pressure (IOP). In this retrospective study, 122 healthy eyes of 62 presbyopic patients, mostly myopic, were divided into two groups. Two distinct asymmetric corneal ablations were applied in peripheral presbyopia correction to produce central-symmetric corneal thickness, which reduces the off-centered corneal shift by utilizing intraocular pressure. The first method used a 90° angled combination in group 1 and the second method used a 45° angled combination in group 2. Target refraction was spherical equivalent of − 1D. Self-developed image processing algorithm analyzed the change in thickness and the posterior cone, and obtained two factors: central symmetry (f) and visual axis deviation (d), from each eye's pre and postoperative maps of Orbscan II. UDVA and UNVA were also analyzed. In both groups, mean SE was about − 1D and there was no significant difference in UDVA. UNVA was better in group 2 than group 1. Only in group 2, corneal thickness and posterior cone became central-symmetric and the posterior corneal apex point relocated towards the visual axis. The p values were 0.03, 0.04, and 0.03, respectively. This is the first study to control corneal shape by utilizing the interaction between intraocular pressure and corneal thickness. Only group 2 was applied with asymmetric corneal ablation created by the 45° angled combination of semi-cylindrical ablation patterns, and intraocular pressure contributed significantly to reduce the off-centered corneal shift and reshaped the posterior corneal cone to the center.

Keywords Asymmetric corneal ablation · Semi-cylindrical ablation · Central-symmetric corneal thickness · Laser asymmetric keratectomy

Introduction

The corneal shape is determined by a complex interaction between biomechanical properties such as corneal thickness and stiffness as well as intraocular pressure (IOP) [1, 2]. The corneal thickness is mainly determined by the stroma, which is formed by lamellae, i.e., the flattened layers of collagen fibrils of about 1.5–2.5 μm in thickness [3–5]. In the center of a normal cornea, there are about 300 lamellae and the number of lamellae gradually increases up to about 500 at the limbus [6, 7]. On the other hand, the biomechanical strength of the cornea is due to the arrangement of lamellae [4]. The corneal center adopts a preferred meridional orientation in the center and undergoes a smooth transition into a circumferential arrangement at the limbus [8–10]. Recent studies claim that this change in orientation from meridional at the center to circumferential at the limbus results in a decrease in corneal stiffness in the peripheral area [11]. This fact may enhance corneal distortion in the mid-peripheral and peripheral area due to changes in IOP [2]. After refractive surgery, however, it has been shown that a hypocellular primitive stromal scar in the flap interface weakens the central and paracentral cornea [12, 13] leading to a further steepening in the central part than in the periphery [14].

Recently, there has been an increasing interest in understanding how corneal refractive surgery induces changes in

✉ José Alberto Rodríguez Agudo
jose.a.rodriguez@fau.de

Jinyoung Park
jinyoung.park@fau.de

Jina Park
jinaa.park@mail.utoronto.ca

Seongsu Lee
Issoph@hanmail.net

Kisung Park
cnear@naver.com

[1] Institute of Fluid Mechanics, University of Erlangen-Nuremberg, Campus Busan, Busan, Republic of Korea

[2] ShapeVision Co., Hwaseong City, Republic of Korea

[3] Lee Seongsu Eye Center, Jinju, Republic of Korea

the biomechanics of the cornea [15–18] with its corresponding impact on the postoperative corneal shape. Ortiz et al. (2007), for instance, observed a significant decrease in IOP and biomechanical properties in postoperative laser in situ keratomileusis (LASIK) eyes [19]. These biomechanical changes in the cornea, that may be derived from the LASIK flap [19, 20], induce significant changes in aberrations [21]. Despite the fact that most corneal changes occur on the anterior cornea, the posterior cornea may also change after refractive surgery due to changes in intraocular pressure or postoperative corneal thinning [22]. The forward shift of the posterior corneal surface after photorefractive keratectomy (PRK) and LASIK was first documented in literature using slit-scanning topography [23–26]. Although other authors using Scheimpflug photography pointed to a minor change in posterior corneal elevation [27–29], recent studies suggest again a significant forward protrusion of the posterior cornea after femtosecond laser-assisted LASIK and PRK [14, 30]. Apart from serious postoperative complications such as iatrogenic keratectasia [25, 31, 32], corneal shift induces myopic regression after laser refractive surgery [33]. A postoperative increase in higher-order aberrations (HOA) is indeed associated with standard refractive surgeries [33–38]. It is clear that for a proper prediction on how the cornea evolves after refractive surgery, an exhaustive in vivo rheological analysis is required. Up to this day, however, it still remains one of the greatest challenges of modern rheometry.

In order to correct distorted corneal shape without considering the complex factors of corneal changes as described above, we developed the hypothesis that a central-symmetric corneal thickness leads intraocular pressure into reducing the off-centered posterior corneal shift and relocating the posterior cone to the corneal center. As beneficial outcomes, the posterior apex point progressively relocates to align with the visual axis, and the irregular posterior curvature and central-symmetric corneal curvature deviation progressively improves. For illustrative purposes, distorted and ideal corneas with its corresponding corneal posterior elevation maps are presented in Fig. 1.

The posterior corneal apex zone is shown as a posterior corneal cone in the map of Orbscan II. We define the cause of corneal distortion as off-centered corneal shift produced by intraocular pressure. The thickness deviation of the cornea, represented by δT_i, is defined as the absolute difference between the corneal thickness at a certain angle i and at its supplementary angle $i + 180$, evaluated in the 3–5-mm zone. Accordingly, $\delta T_i = abs(thickness_{i^\circ} - thickness_{i+180^\circ})$. This definition matches the so-called central symmetry deviation. For example, in Fig. 1, the thickness deviation is evaluated between 0 and 180°. The size of the asymmetrical shape and the possibility of corneal distortion occurring from intraocular pressure increase when the thickness deviation in central symmetry increases, as illustrated in the left part of Fig. 1. On the other hand, there is more tendencies for the cornea to be a symmetric shape when the thickness deviation in central symmetry decreases, as illustrated in the right part of Fig. 1. This figure explains that corneal shape is determined by an ongoing

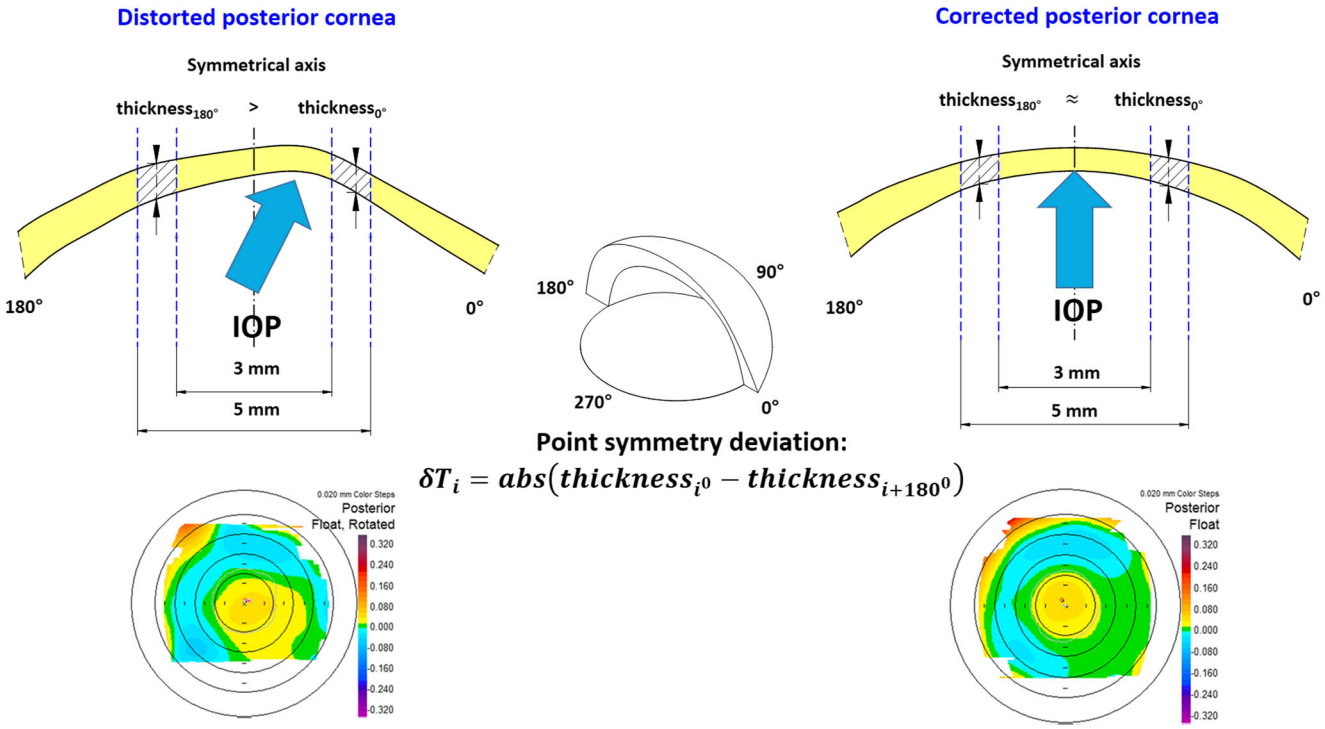

Fig. 1 Illustration of distorted corneal shape (top-left) and ideal corneal shape (top-right). Distorted posterior corneal elevation map (bottom-left) and ideal posterior corneal elevation map (bottom-right) are presented at the bottom of the figure

interaction between corneal thickness distribution and intraocular pressure, and it matches our hypothesis.

Materials and method

A new laser corneal ablation method, laser asymmetric keratectomy (LAK), was developed to establish and implement the hypothesis. The corneal ablation plans required for LAK were designed by a self-developed software (Vision-Up).

A commercially available Argon Fluoride (ArF) ISOD200 excimer laser device (Kera Harvest Inc.) with a wavelength of 193 nm was used for LAK implementation. This laser system has dual spot sizes of approximately 0.63 $mm^2 \pm 20\%$, maximum repetition rates of 300 Hz, fluence range of 100–180 mJ/cm^2, energy pulse of less than 1 mJ and uses a 300-Hz passive-type eye tracking function. Table 1 shows the laser specifications.

LAK implementation is based on a standard laser ablation method for correcting astigmatism that consists of axisymmetric cylindrical ablation patterns as depicted in Fig. 2d. That method was slightly modified to create asymmetric corneal ablations as shown in Fig. 2a in order to reduce the thickness deviation in central symmetry. The self-developed software permitted the ophthalmic surgeons to execute LAK with the aforementioned standard laser system after the confirmation of central-symmetric thickness deviation of the target cornea. The final goal of LAK is to minimize the postoperative corneal thickness deviation in central symmetry without any changes to pre and postoperative mean curvature value in the cornea.

Figure 2 illustrates the method. The asymmetric ablation patterns are created by various combinations of semi-cylindrical ablation patterns (see Fig. 2b, c). The software Vision-Up requires the data for refractive errors and corneal thickness distribution, to produce an asymmetric corneal ablation plan for executing LAK. Figure 2d shows that a pair of axisymmetric semi-cylindrical ablation patterns, which is used to correct astigmatism in current laser vision correction, is unnecessary in LAK execution.

Table 1 Laser specifications

Laser class	4
Laser model	ArF excimer laser [193 nm]
Spot size	0.9×0.7 mm ± 20%
Fluence	100–180 mJ/cm^2 (on cornea)
Energy per pulse	< 1 mJ (on cornea)
Purse duration	21–26 μs (on cornea)
Pulse width	4–15 ns
Repetition rate	Max. 300 Hz
Ablation method	Random/fractal ablation, dual laser beam
Adjustable optical zone	Φ 3~8 mm
Eye tracking	300 Hz (passive type)

When LAK is executed, the refractive power of the cornea is changed through a partial corneal curvature change. In the hypothesis, after the execution of LAK, corneal curvature and shape become balanced in central symmetry, but it is impossible to recover the refractive power change. Thus, it is required to find a way to calculate the changed refractive power and be able to offset it, in order to control visual acuity. The ablation pattern used in LAK uses the Spherical Equivalent Refraction formula (SER formula) to solve this challenge. Here, the change in refractive power (Δ) refers to the difference in refractive power before and after corneal ablation executed with LAK. Figure 2a, d shows that a semi-cylindrical corneal ablation is equivalent to a one-sided cylindrical corneal ablation. Thus, the change in refractive power produced by semi-cylindrical corneal ablation is equivalent to half of the change in refractive power produced by cylindrical ablation. According to the SER formula, the change in refractive power produced by cylindrical aberration is equivalent to half of the change in refractive power produced by spherical aberration. Thus, the change in refractive power produced by semi-cylindrical corneal ablation is equivalent to a quarter of the change in refractive power produced by spherical ablation. Therefore, the change of the total refractive power (Δ) produced by LAK can be calculated by multiplying the sum of the semi-cylindrical ablation patterns by 0.25D spherical. For instance, in Fig. 2d, it shows the laser ablation pattern for correcting the cornea of cylindrical + 1D with axis 180°. It makes a change of − 0.5D spherical in corneal refraction. In Fig. 2b, the sum of semi-cylindrical corneal ablation patterns is the same as the sum of semi-cylindrical corneal ablation patterns in Fig. 2d. Therefore, it can be assumed that the change of − 0.5D spherical in corneal refraction occurs when the ablation pattern in Fig. 2b is executed. In Fig. 2c, the sum of the semi-cylindrical corneal ablation patterns is 1.5 times larger than in Fig. 2b, d. It can be thus assumed that the change of − 0.75D spherical in refraction occurs when Fig. 2c is performed. Also, the change in refractive powers by the execution shown in Fig. 2b, c can be eliminated by laser ablation for correcting − 0.5D and − 0.75D spherical, respectively. As a result, the change in corneal refractive power is not caused by LAK. Accordingly, this brings us to an important statement: LAK can be performed in combination with other vision correction methods including current laser vision correction and laser presbyopia correction.

In this retrospective study, peripheral presbyopia correction with asymmetric corneal ablation (PPA correction) was applied on patients and an outcome analysis was performed on 122 healthy presbyopic eyes of 62 presbyopia patients (mean age of 48.81 ± 4.50 years and SE of − 3.51 ± 2.14D). Patients were mostly myopia, with some emmetropia who experienced

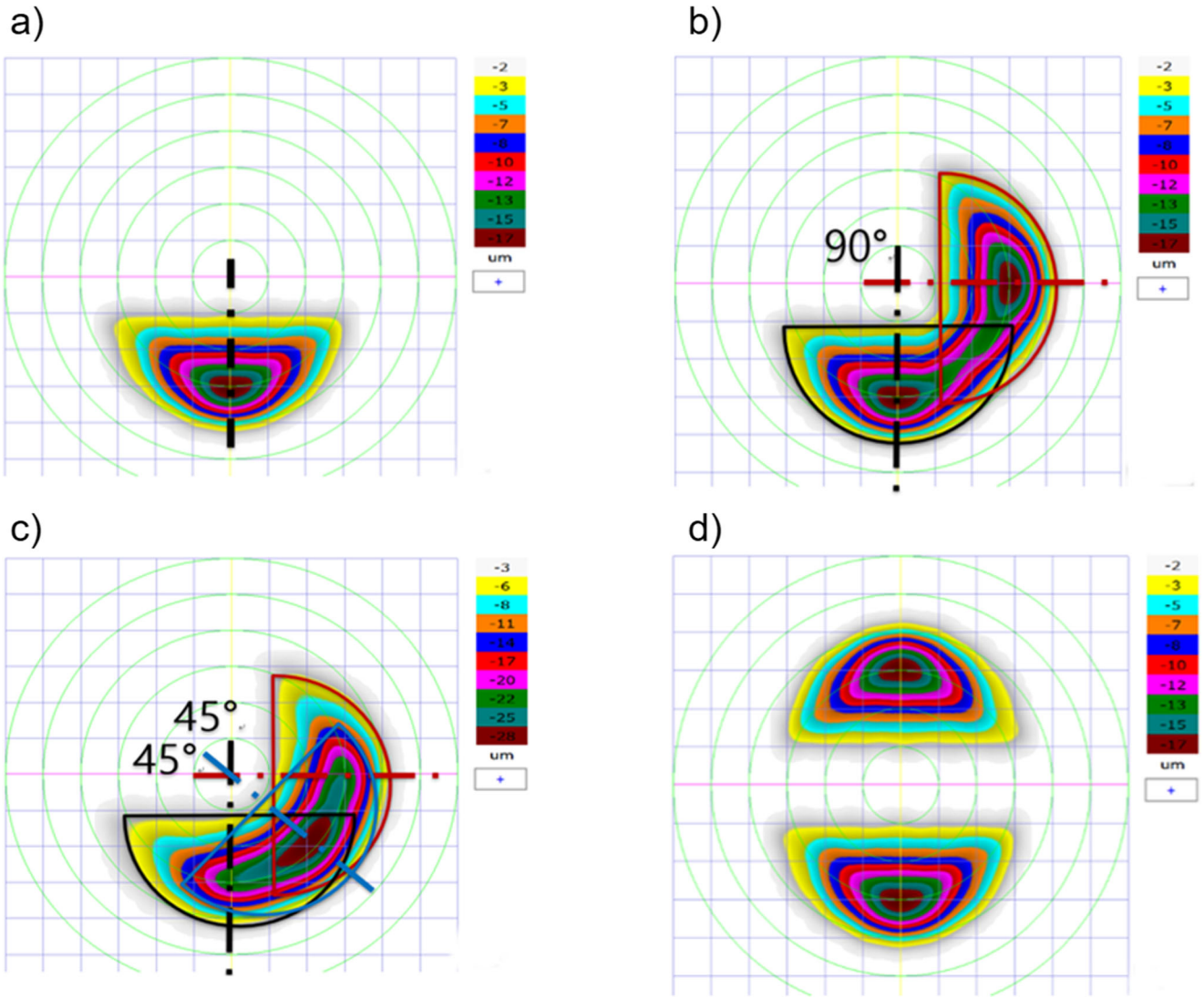

Fig. 2 Simple examples to illustrate laser corneal ablation patterns. **a** A basic semi-cylindrical ablation pattern. **b** An asymmetric ablation pattern created by a 90° angled combination of two semi-cylindrical ablation patterns. **c** An asymmetric ablation pattern created by a 45° angled combination of three semi-cylindrical ablation patterns. **d** An axisymmetric cylindrical ablation pattern to correct + 1D astigmatism that is composed of multiple semi-cylindrical ablation patterns that are equivalent

laser myopia correction in the past. They were divided into two groups according to the duration of the operation, and different LAK techniques were applied to each group. Group 1 was formed by 42 normal subjects, treated between 2013 and 2014, with an average age of 50.10 ± 4.22 years, a mean SE of − 3.63 ± 2.30D, UDVA of 0.35 ± 0.30, and UNVA of 0.44 ± 0.28. Group 2 was formed by 20 normal subjects, treated between 2016 and 2017, with an average age of 46.10 ± 3.92 years, a mean SE of − 3.24 ± 1.75D, UDVA of 0.40 ± 0.29, and UNVA of 0.56 ± 0.26.

PPA correction has a dual corneal ablation process consisting of LAK and peripheral presbyopia correction (PP correction). The goal of PP correction is to produce a naked eye that is able to see distance through central cornea and has a reading-glasses effect through peripheral cornea. The goal of LAK is to convert corneal thickness into central symmetry, reduce off-centered corneal shift, and relocate posterior corneal cone into the center utilizing intraocular pressure. The target of PPA correction is to achieve both goals for PP correction and LAK, and the target refraction is to achieve postoperative SE of − 1D. Group 1 patients were treated with the initial method of LAK (Initial LAK). This method used asymmetric ablation patterns that were produced by the 90° angled combination of semi-cylindrical ablation patterns. Group 2 patients were treated with the advanced method of LAK (Advanced LAK). This method used asymmetric ablation patterns that were produced by the 45° angled combination of semi-cylindrical ablation patterns. Target patients were either myopia or emmetropia, consisting of only those who had been treated with laser myopia correction in the past. The

Table 2 Patients' preoperative demographics

	Group 1 ($n = 84$)	Group 2 ($n = 38$)	p value
Age (years)	–	–	–
Mean ± SD	50.10 ± 4.22	46.10 ± 3.92	–
Range	42 to 57	40 to 60	–
Refractive error	–	–	0.2
Mean ± SD	− 3.63 ± 2.30	− 3.24 ± 1.75	–
Range	− 8.25 to (+)0.75	− 5.9 to (+)0.5	–
Preoperative UDVA	–	–	–
Mean ± SD	0.35 ± 0.30	0.40 ± 0.29	–
Range	0.01 to 1.0	0.05 to 1.0	–
Preoperative UNVA	–	–	–
Mean ± SD	0.44 ± 0.28	0.56 ± 0.26	–
Range	0.1 to 1.0	0.1 to 1.0	–
Central symmetry (f)	–	–	0.7
Mean ± SD	0.32 ± 0.16	0.33 ± 0.17	–
Range	0.01 to 0.77	0.05 to 0.64	–
Visual axis deviation (d)	–	–	0.3
Mean ± SD	0.21 ± 0.11	0.20 ± 0.11	–
Range	0.03 to 0.56	0.02 to 0.49	–

demographics of this retrospective study is summarized in Table 2. The eye surgery was performed at Lee Seong Su Eye Center located in Jinju, Republic of Korea, in accordance with the tenets of the Declaration of Helsinki. The National Bioethics Committee in Seoul, Republic of South Korea, stated that no IRB approval was required for the retrospective analysis of the data. UDVA was measured at 3 m distance and UNVA was measured at 35 cm distance using *Han Chun Suk distance visual acuity chart* and *Han Chun Suk near visual acuity chart*, respectively. The refractive errors of patients were measured by cycloplegic refraction methods and inputted into Vision-Up along with the information from the thickness map obtained using Orbscan II.

For analyzing the corneal shape progression, a self-developed image processing algorithm was applied to calculate the central symmetry thickness deviation. The algorithm also obtained two factors: central symmetry (f) and visual axis deviation (d), from Orbscan II maps at the preoperative stage and at 3, 6, and 12 postoperative months for each eye treated with PPA correction. Both factors were stored in a database for further statistical analysis. The same algorithm calculated the mean value and the standard deviation in relation to the thickness distribution, posterior cone, and the alignment between the posterior apex point and the visual axis in cornea. The differences between the data from the same population were evaluated based on Wilcoxon rank-sum test. The outcomes between different groups were compared using the Student's t test. Normality of the data was evaluated with the Kolmogorov-Smirnov test. The level of significance was set at p value of less than 0.05 for each parameter. The algorithm including the statistical analysis was implemented in Matlab®. Additionally, UDVA, UNVA, and SE were also analyzed.

From this point on, we would like to use pre and postoperative maps of a sample patient's cornea and the simulation of laser corneal ablation process to explain the execution of LAK and PPA correction, as well as its outcome analysis. The refractive error of the sample patient eye was − 5.75D spherical and − 0.25D cylindrical with axis 97° preoperatively. PPA operation was performed to her on February 2014. Her astigmatism was ignored in the correction process.

Figure 3 is a sketch to explain the process of LAK on the sample patient's cornea. Figure 3a shows the preoperative thickness of her cornea. Figure 3b shows her expected postoperative thickness computed in Vision-Up. Figure 3c shows her actual postoperative residual thickness at the first postoperative year. In Fig. 3, black and blue values represent corneal thickness, and red values represent central symmetry thickness deviation, in microns. The data in Fig. 3a, c were

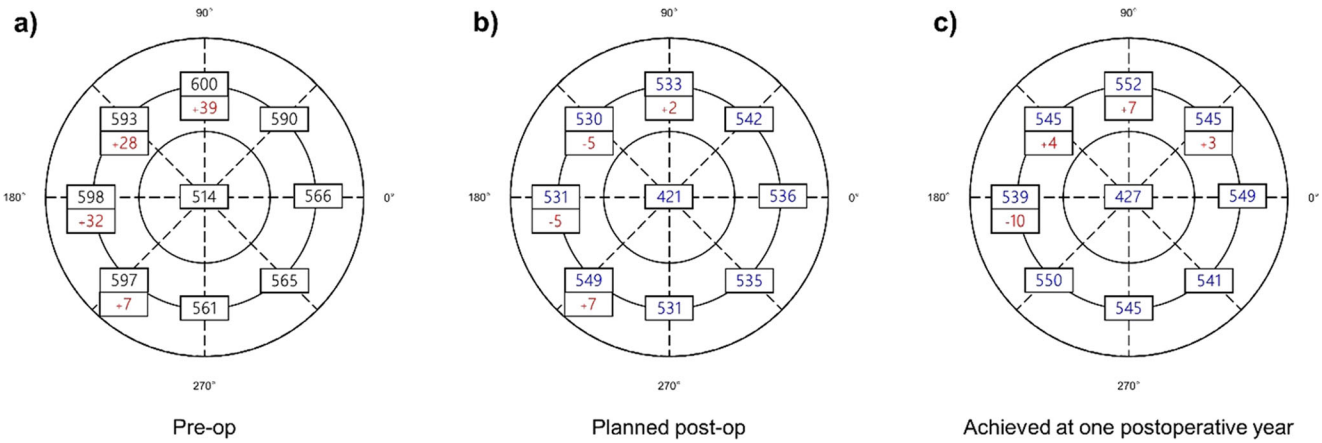

Fig. 3 Sketch of corneal thickness. **a** Preoperative thickness of the sample patient; **b** expected postoperative thickness calculated by Vision-Up software; and **c** actual postoperative thickness of the sample patient. Values are represented in microns. The circles correspond to 3 mm zone, 5 mm zone, and 7 mm zone, from the inside to the outside

measured with slit-scanning technology using Orbscan II (Bausch & Lomb, USA).

Preoperatively, the nasal side of the sample patient's cornea appeared to be thicker by + 39 μm at 90°, + 28 μm at 135°, + 32 μm at 180°, and + 7 μm at 225° in central symmetry as depicted in Fig. 3a. To correct the corneal thickness into central symmetry as depicted in Fig. 3b, Vision-Up built the laser asymmetric corneal ablation code: OS090-40. As depicted in Fig. 3c, central-symmetric thickness deviation is reduced at the first postoperative year, after executing laser corneal ablation by OS090-40.

Figure 4 is a simulation to explain PPA correction for the sample patient's corneal ablation in detail. Figure 4a demonstrates merged laser ablation patterns for PPA correction. It is made by a combination of two different laser ablation processes: PP correction as shown in Fig. 4b and LAK as shown in Fig. 4c. PP correction is made by a combination of two spherical ablation processes as depicted in Fig. 4d, e. Figure 4d shows an ablation pattern to correct − 3.75D spherical, based on a 6.6-mm optical zone with a transition to 7.6 mm. For the sample patient, this ablation using the ArF excimer laser as described in Table 2, with a laser shot frequency of 250 Hz

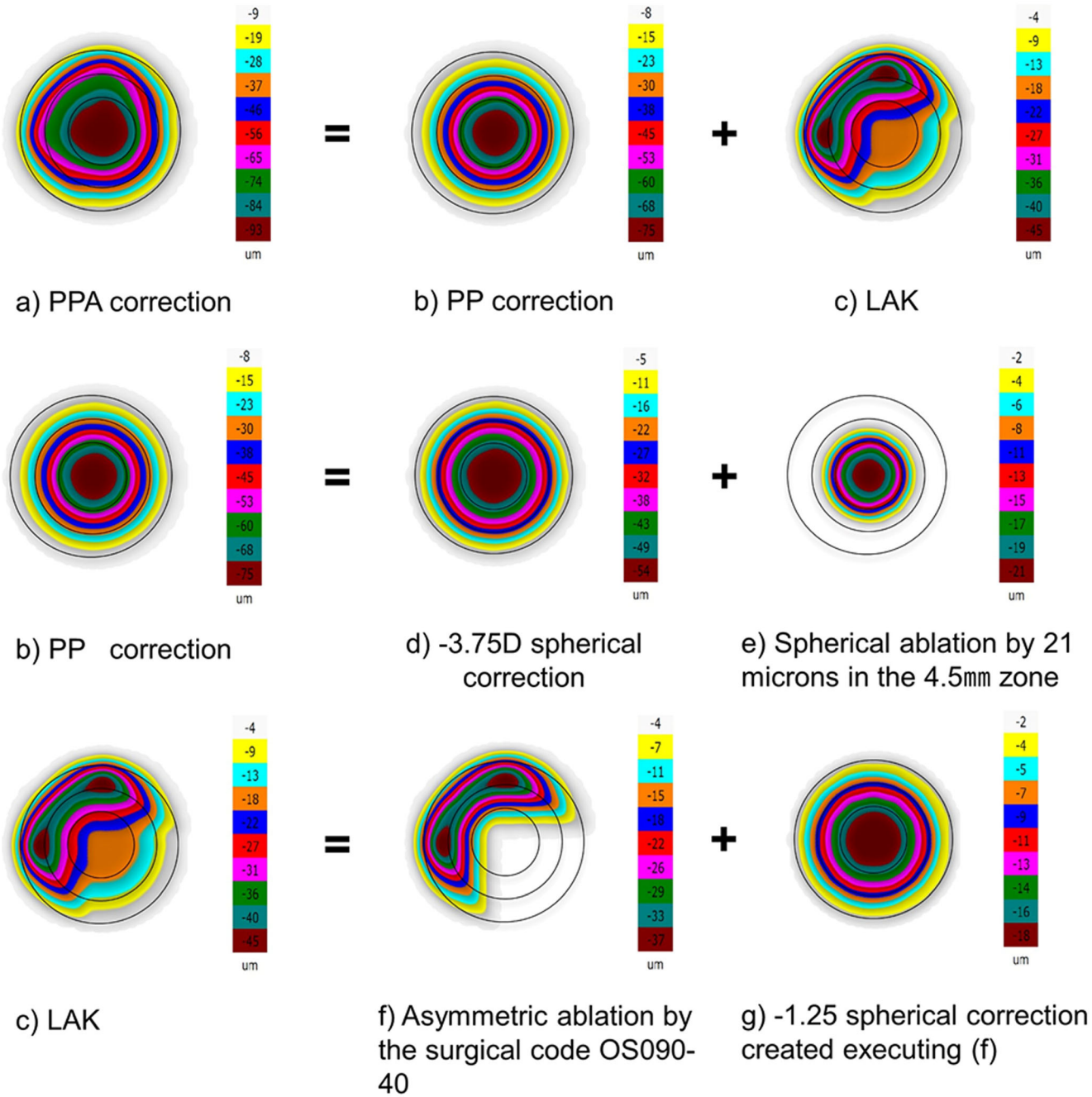

Fig. 4 Actual simulations of laser ablation patterns for PPA execution on sample patient's cornea

took 29 s. Figure 4e shows an ablation pattern to eliminate 21 mm progressively from the edge to the center, based on a 4.5-mm optical zone without transition. The time required for this ablation was 4 s. The total time for PP correction ablation was thus 33 s. As shown in Fig. 4d, − 3.75D spherical correction resulted in a − 2D spherical cornea and Fig. 4e shows the correction of − 2D spherical in the corneal center. Figure 4c illustrates merged laser ablation patterns for LAK. It is completed by a combination of two ablation processes, shown in Fig. 4f, g. Figure 4f shows asymmetric ablation according to the asymmetric corneal ablation code OS090-40, which required 13 s. The code was designed by Vision-Up software. Figure 4g shows a spherical ablation created to correct − 1.25D spherical, which required 9 s. Figure 4f shows the process of how central-symmetric corneal thickness are made. Once the cornea is asymmetrically ablated, corneal refraction is changed by corneal curvature change. Figure 4g shows the process of how the change in corneal refraction (Δ) caused by executing the asymmetric corneal ablation code OS090-40 was eliminated. The total time required for LAK ablation was 22 s. The total laser ablation for the complete PPA correction (peripheral presbyopia correction with asymmetric corneal ablation) required 55 s.

Figure 5 illustrates the postoperative tomographic maps of the sample patient's cornea at the preoperative stage and at 3, 6, and 12 months after being treated with PPA correction. According to the maps in Fig. 5, central-symmetric corneal thickness, posterior corneal cone, anterior axial curvature, and posterior axial curvature are continuously improved after the operation.

In the anterior tangential curvature maps in Fig. 6, the maps in panel a show that a ring-shaped curvature is created after PP correction and the maps in panels b and c show that the ring-shaped curvature is well maintained postoperatively. The maps in Figs. 5 and 6 prove the hypothesis that the corneal shape and curvature are improved without any corneal distortion, by utilizing intraocular pressure after LAK.

In this study, for analyzing the pre and postoperative changes in central-symmetric thickness deviation, a self-developed image processing algorithm was used to systematically measure central-symmetric thickness deviation. The algorithm automatically obtained the thickness of the paracentral cornea from Orbscan II maps with a resolution of 1°. Then, it computed the central-symmetric thickness deviation according to the maps of Fig. 5a.

The graphs at the top of Fig. 7 represent central symmetry deviation for the thickness maps preoperatively and at 3, 6, and 12 postoperative months, respectively (see the maps in Fig. 5a). The area under these curves is calculated as $\Delta T = \sum_{i=1}^{180} \delta T_i$. It represents the total central symmetry thickness deviation in micrometer, indicated by ΔT in the figure. As predicted, the total central symmetry deviation for this illustrative example showed a considerable reduction after

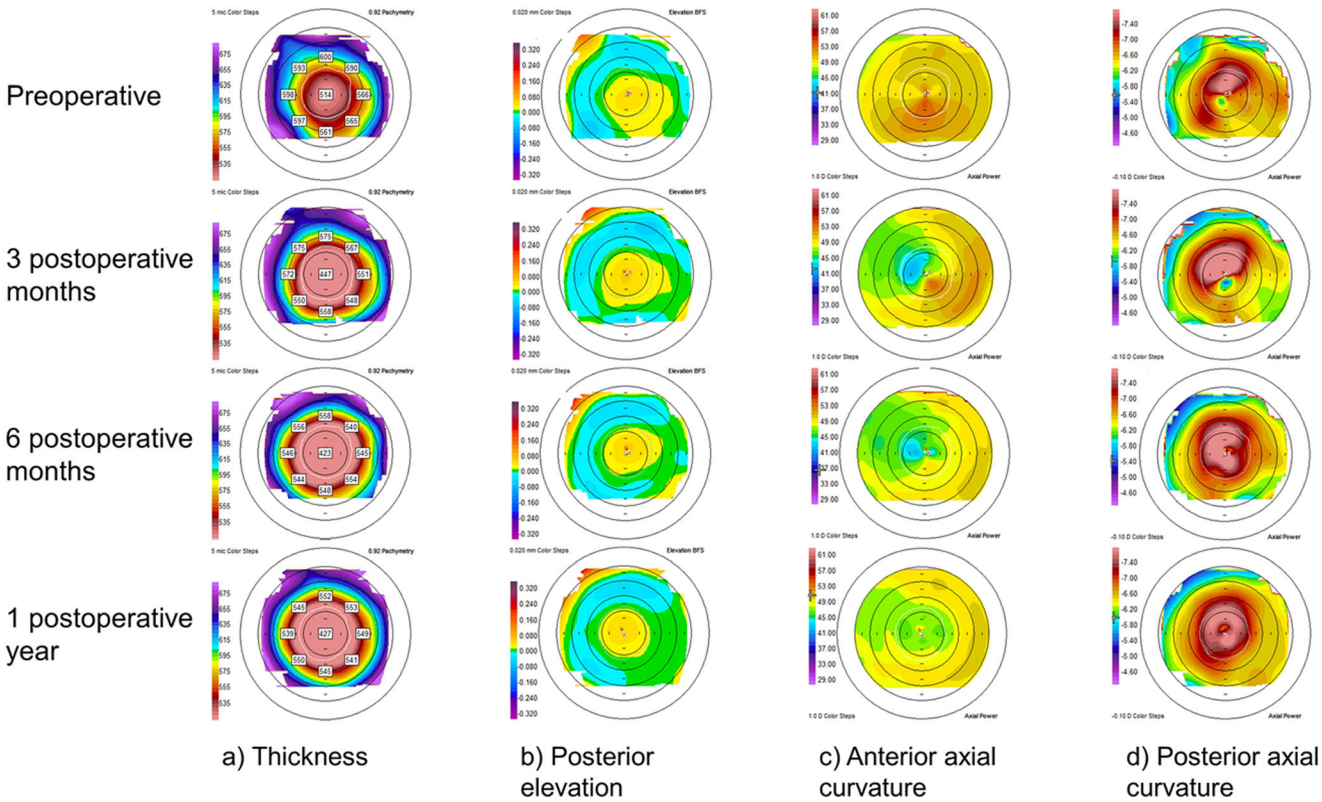

Fig. 5 Orbscan II corneal tomography maps of the sample patient in pre and postoperative PPA correction

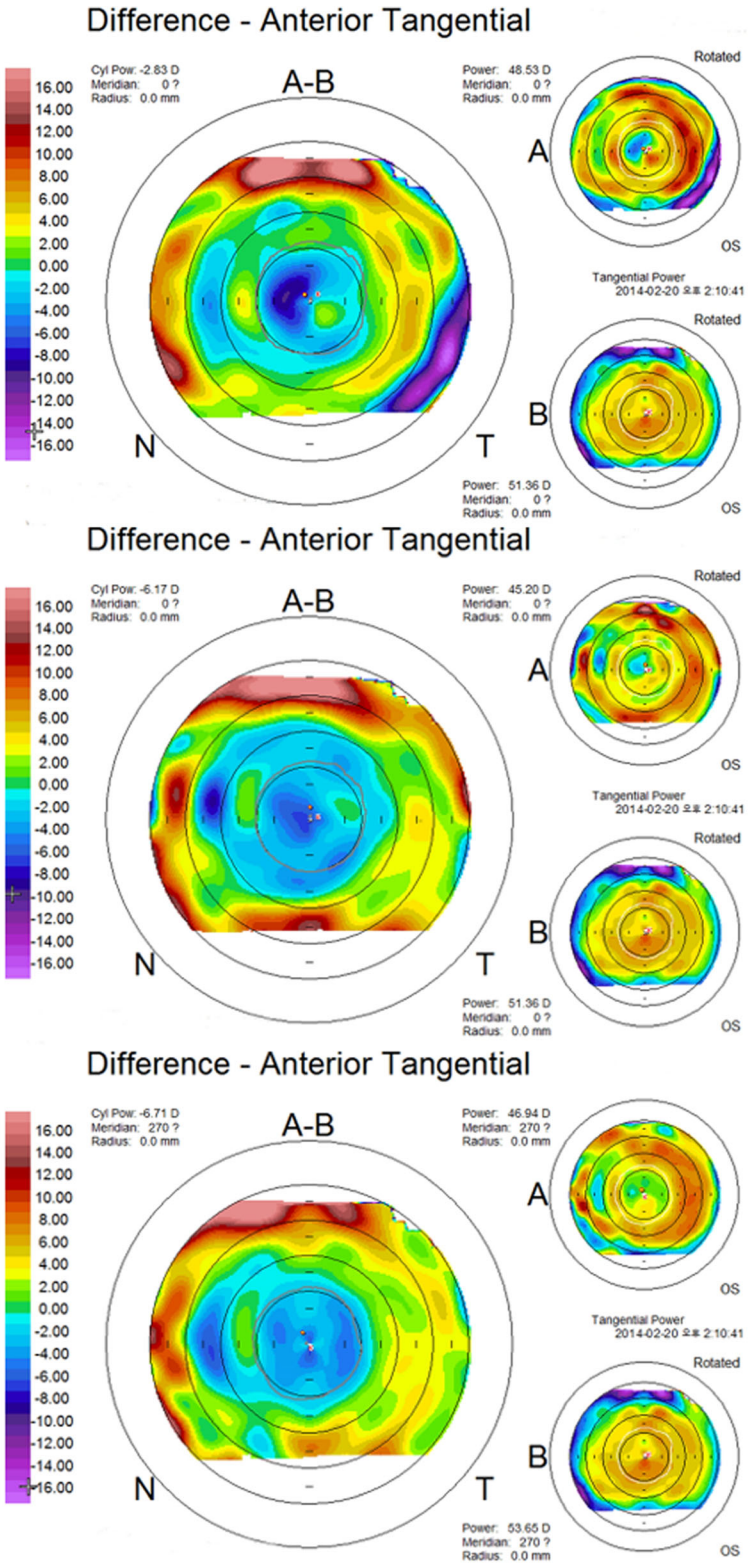

Fig. 6 The comparison of pre and postoperative maps of the same cornea depicted in Fig. 5

the operation. The same image processing routine systematically followed up the posterior corneal shape and position of the central and paracentral zone (0–7 mm) before and after surgery. It used the topographer screen obtained by Orbscan II as input data to identify two normalized parameters that characterize the deviation of posterior corneal cone from central

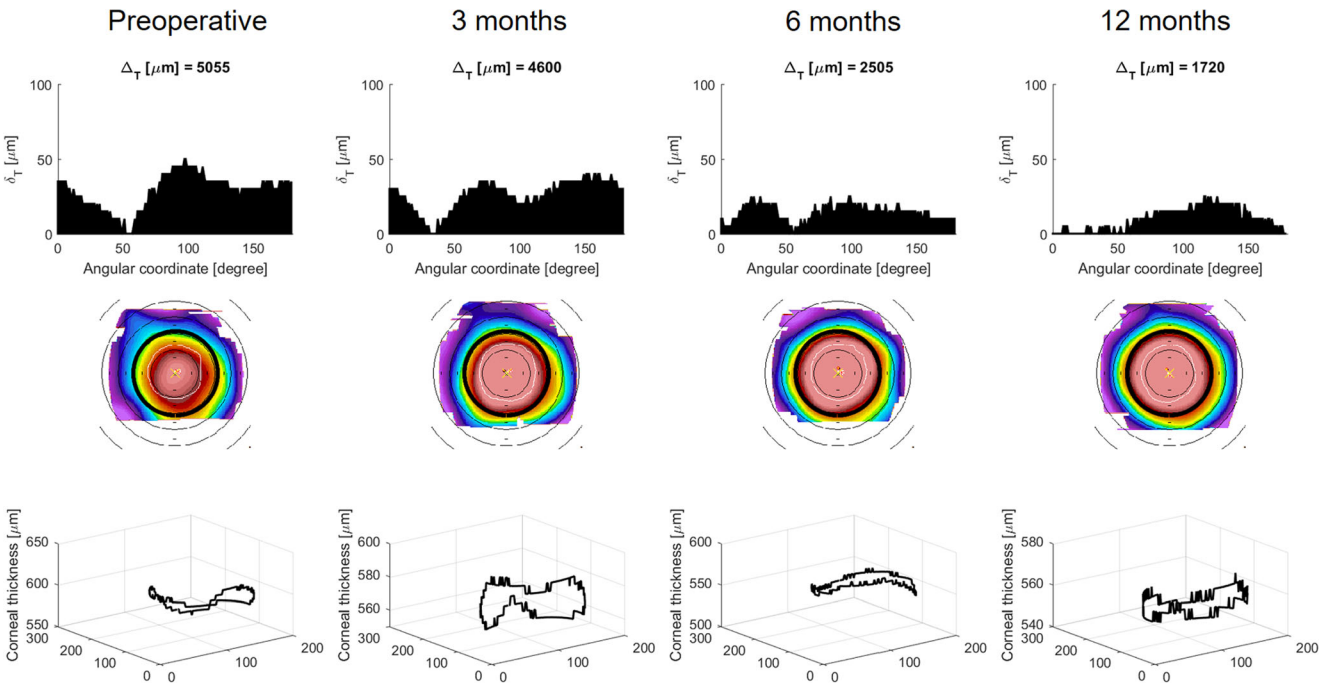

Fig. 7 Central symmetry deviation for the thickness maps preoperatively and at 3, 6, and 12 postoperative months

symmetry, and the alignment between the apex point in posterior corneal cone and the visual axis.

Figure 8 represents the data obtained from the image processing routine for posterior elevation maps in Fig. 5b. The self-developed image processing algorithm first obtains a contour of the posterior corneal cone (shown as a clear yellow area in the maps of Fig. 5b, and an outer black line in Fig. 8). The algorithm also identifies the contour of the posterior corneal apex point in the center. It is represented in Orbscan II maps by a gradation of yellow (see the maps of Fig. 5b). Orbscan II maps are represented within a resolution of 20 μm and the image segmentation is based on a simple red-green-blue intensity thresholding. Subsequently, the code creates a mirror image of the corneal cone that is central-symmetric with respect to the visual axis (see the dotted blue line in Fig. 8). The normalized factor selected to quantify the deviation in central symmetry is defined as the overlapping area between the original corneal cone and its central-symmetric mirror image (see the red line in Fig. 8) divided by the sum of the area of the corneal cone and its mirror image. Accordingly, a central symmetry factor equal to 1 represents a zero deviation in central symmetry, while a factor approaching 0 represents a very high level of deviation. This system permits us to quantify the deviation of corneal thickness in central symmetry, with a single normalized parameter. The central symmetry factor is represented by *f* in the illustrative example of Fig. 8.

The factor *f* gradually increases over time, indicating that the posterior corneal cone tends to adopt a central-symmetric shape after surgery. The evolution in position and size of the cone also provides insight into long-term visual acuity. According to our theory, a reduction in central-symmetric thickness deviation leads the posterior corneal apex point close to the visual axis, by reshaping the posterior corneal cone into

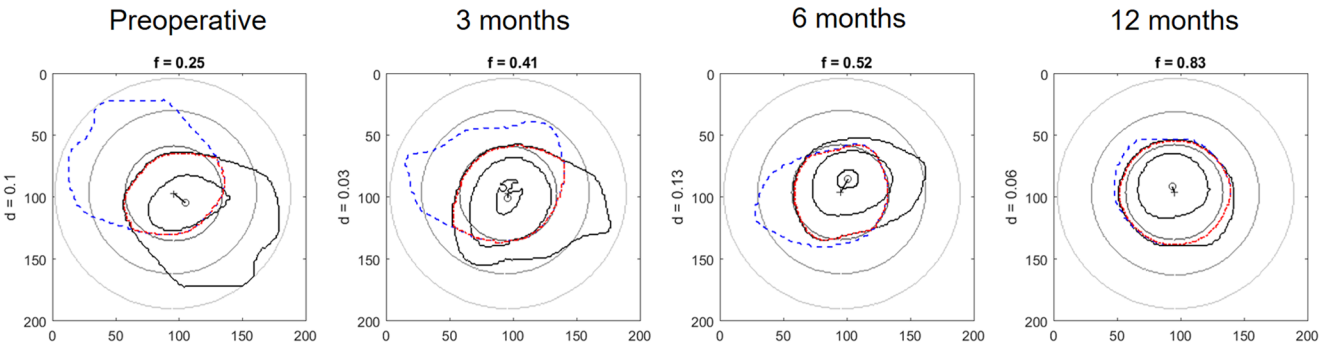

Fig. 8 Output data obtained after applying the posterior corneal cone's image processing routine in the maps as depicted in Fig. 5b. The central symmetry deviation factor, *f*, and the visual axis center deviation factor, *d*, are represented in the top and the left side of each snapshot, respectively

the center using intraocular pressure. To clarify this, the algorithm determines the centroid of the most elevated region of the posterior cornea and measures the distance from this point to the visual axis center. The normalized factor is obtained as the ratio between this distance and the equivalent diameter of the cone based on its surface area. The deviation factor of the visual axis center is represented by *d* in the example of Fig. 8. The sample patient's eye has maintained postoperative refraction between SE of − 1.0D and − 1.25D at the first postoperative year. As well, the thickness map at one postoperative year of Fig. 5a reveals corneal thickness deviation of + 7 μm at 90°, + 4 μm at 135°, − 10 μm at 180°, and − 3 μm at 225°, which is similar to what was expected before surgery (see the sketch in Fig. 3b). The central symmetry thickness deviation has been successfully minimized when compared to her preoperative conditions; from $\Delta T = 5055$ μm preoperatively to $\Delta T = 1720$ μm at one postoperative year. At the first postoperative year, the central symmetry factor, *f*, was 0.83, being close to 1 (see Fig. 8). This indicates a definite improvement in her posterior corneal cone in terms of central symmetry. In addition, the posterior corneal apex center in the posterior cone gradually relocated towards the visual axis center. At one postoperative year, *d* approached zero as shown in Fig. 8. Lastly, the patient's cornea has been experiencing an improvement of posterior irregular curvature as demonstrated in the posterior axial curvature maps of Fig. 5d.

Results

In this retrospective study, the patients were divided into two groups according to the surgical method and the outcome analysis. Eighty-four eyes of 42 patients (mean age of 50.10 ± 4.22 years; UDVA of 0.35 ± 0.30; UNVA of 0.44 ± 0.28) were in group 1, and 38 eyes of 20 patients (mean age of 46.10 ± 3.92 years; UDVA of 0.40 ± 0.29; UNVA of 0.56 ± 0.26) were in group 2. Preoperative SE in group 1 was − 3.63 ± 2.30D, and postoperative SE in group 1 was − 1.00 ± 0.69D at 1 month, − 1.05 ± 0.58D at 3 months, − 1.05 ± 0.57D at 6 months, and − 1.04 ± 0.61D at 1 year. Preoperative SE in group 2 was − 3.24 ± 1.75D, and postoperative SE in group 2 was − 1.24 ± 0.77D at 1 month, − 1.11 ± 0.58D at 3 months, − 1.17 ± 0.42D at 6 months, and − 1.15 ± 0.50D at 1 year. The patients in group 1 were treated with Initial LAK between 2013 and 2014. The patients in group 2 were treated with Advanced LAK between 2016 and 2017. For group 1, the central-symmetric thickness deviation obtained from the image processing routine, as depicted in Fig. 7, resulted in $\Delta T = 4626 \pm 1804$ μm preoperatively, and $\Delta T = 4507 \pm 2815$ μm, $\Delta T = 4749 \pm 2583$ μm, and $\Delta T = 4842 \pm 1600$ μm at 3, 6, and 12 postoperative months, respectively. For group 2, the central-symmetric thickness deviation was $\Delta T = 4568 \pm 1636$ μm preoperatively, and $\Delta T = 3834 \pm 2611$ μm, $\Delta T = 3603 \pm 1922$ μm, and $\Delta T = 3200 \pm 1981$ μm at 3, 6, and 12 postoperative months, respectively. Preoperatively, there was no statistical difference in the central symmetry factor between the two groups of patients ($p = 0.8643$). The statistical analysis failed to reject the null hypothesis level. The *p* value resulted in 0.1677, 0.5846, and 0.6146, when comparing preoperative central-symmetric thickness deviation with postoperative data at 3, 6, and 12 months, respectively. Therefore, no thickness improvement in central symmetry was observed in group 1, indicating that the ablation procedure failed to obtain a central-symmetric corneal shape. On the other hand, a statistically significant decrease was observed in group 2 at the third postoperative month. The *p* value resulted in 0.0329, 0.0332, and 0.0267 when comparing preoperative central-symmetric thickness deviation with postoperative data at 3, 6, and 12 months, respectively. Advanced asymmetric ablation performed to group 2 patients successfully achieved corneal correction in terms of central-symmetric corneal thickness.

Figure 9 illustrates the central symmetry factor, *f*, for preoperative eyes and its progression over a period of 12 months for group 1 and group 2, respectively. The size of

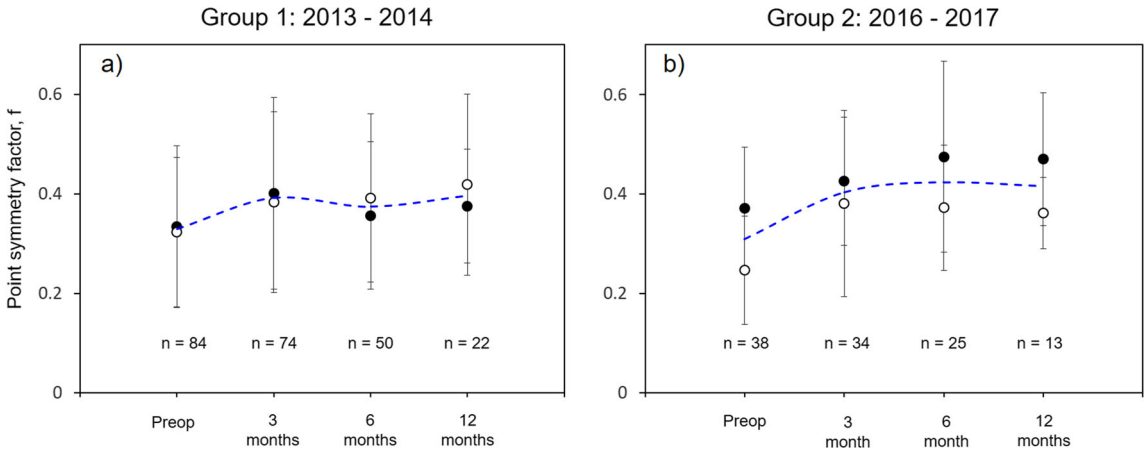

Fig. 9 Progression of the central symmetry factor in group 1 and group 2 over 12 months. Solid and open symbols represent right and left eyes, respectively. The error bars represent the standard deviation of the results

postoperative analyzed eyes is shown under the symbols. Not all of the patients appeared for postoperative inspection during this retrospective study, and the analyzed sample size thus decreased with time. The blue dotted line depicts the average value of the right and left eyes. Preoperatively, there is no statistical difference in the central symmetry factor between the two groups of patients ($p = 0.7490$). In both groups, an increase in the mean central symmetry factor with respect to their preoperative conditions is observed after 3 months. From 3 to 12 postoperative months, the central symmetry factor seemed to stay constant in both groups. For group 1, the statistical comparison between preoperative and postoperative data failed to reject the null hypothesis. The p values resulted in 0.0506, 0.1059, and 0.084 when preoperative central symmetry factors were compared with postoperative data at 3, 6, and 12 months, respectively. For group 2, the increase in the mean central symmetry factor, f, was approximately 32% when compared to their preoperative conditions. In this case, a statistically significant increase in the central symmetry factor was observed. The Wilcoxon test revealed p values of 0.0425, 0.0084, and 0.0207 when postoperative corneal shape at 3, 6, and 12 months was compared with the preoperative one. The statistical comparison between postoperative data revealed no significant change in the central symmetry factor. Figure 7 indeed shows a constant plateau on f for the postoperative results of patients in both groups. This indicates that the corneal shape is mainly changed after 3 months and is sustained with time after the operation.

Figure 10 shows the progression of the visual axis deviation factor, d, for group 1 and group 2, respectively. The number of the analyzed postoperative eyes is shown under the symbols. The blue dotted line represents the average value between right and left eyes. Preoperatively, there was no statistical difference in d between group 1 and group 2 ($p = 0.3445$). For group 1, the mean deviation hardly decreased over the 12 months. The statistical analysis revealed no significant difference between preoperative and postoperative data. The p values resulted in 0.2790, 0.3741, and 0.1823 when preoperative deviation factors were compared with postoperative data at 3, 6, and 12 months, respectively. For group 2, the mean deviation showed a progressive decrease over time, achieving a plateau after 6 months with a maximum decrease of approximately 21%. In this case, the statistical analysis revealed a significant decrease in d after only 3 months (p value = 0.0340). In group 2, there was a high tendency for the posterior corneal cone to get relocated closer to the visual axis center than group 1. In addition, the changes of UDVA, UNVA, and posterior corneal curvature of the patients in group 1 and group 2 were reviewed separately.

Figure 11a illustrates the outcomes in cumulative UDVA of group 1 (gray bars) and group 2 (green bars). At the first postoperative year, 78% of patients in group 1 achieved UDVA of 20/25 or better, while 89% of patients in group 2 achieved UDVA of 20/25 or better. The progression in postoperative mean UDVA over 1 year is represented in Fig. 11b. Visual acuity is stated in LogMAR format and the error bars represent standard deviation. Solid and open symbols depict the outcomes in terms of the mean UDVA (LogMAR) and the mean UNVA (LogMAR) data for group 1 and group 2, respectively. The mean UDVA is 0.05 ± 0.19 (LogMAR) and 0.03 ± 0.13 (LogMAR) for group 1 and group 2, respectively. As shown in Fig. 11b, patients' UDVA remains mostly constant during a follow-up of 12 postoperative months. The statistical comparison between group 1 and group 2 postoperative outcomes reveal no significant difference.

The outcomes for near vision visual acuity are represented in Fig. 12a as a cumulative distribution. At the first postoperative year, 53% of the patients in group 1 (gray bars) had UNVA of J3 (20/40) or better, while 100% of the patients in group 2 (green bars) had UNVA of J3 (20/40) or better. Figure 12b shows the progression of the mean UNVA over

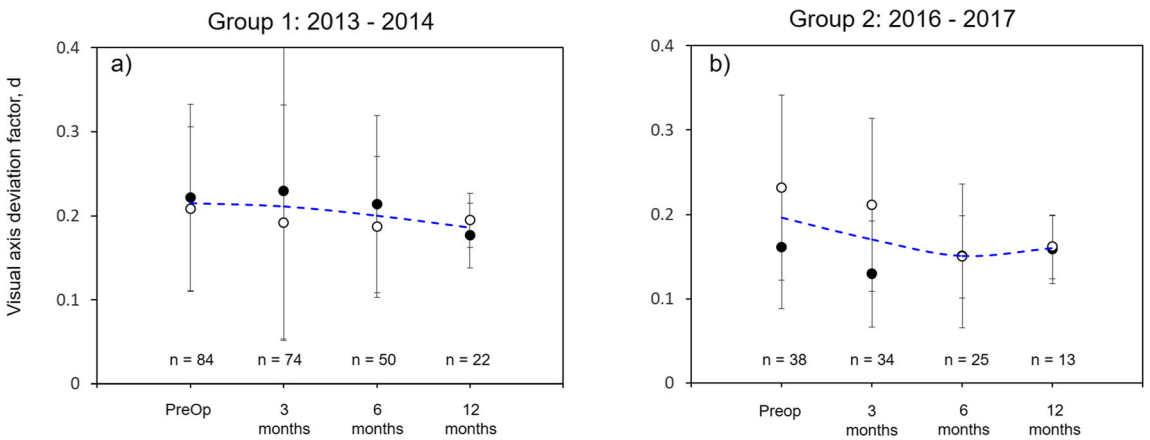

Fig. 10 Progression of the deviation between the apex centroid of posterior cornea and the visual axis center in group 1 and group 2 over 12 months. Solid and open symbols represent right and left eyes, respectively. The error bars represent the standard deviation of the measurements

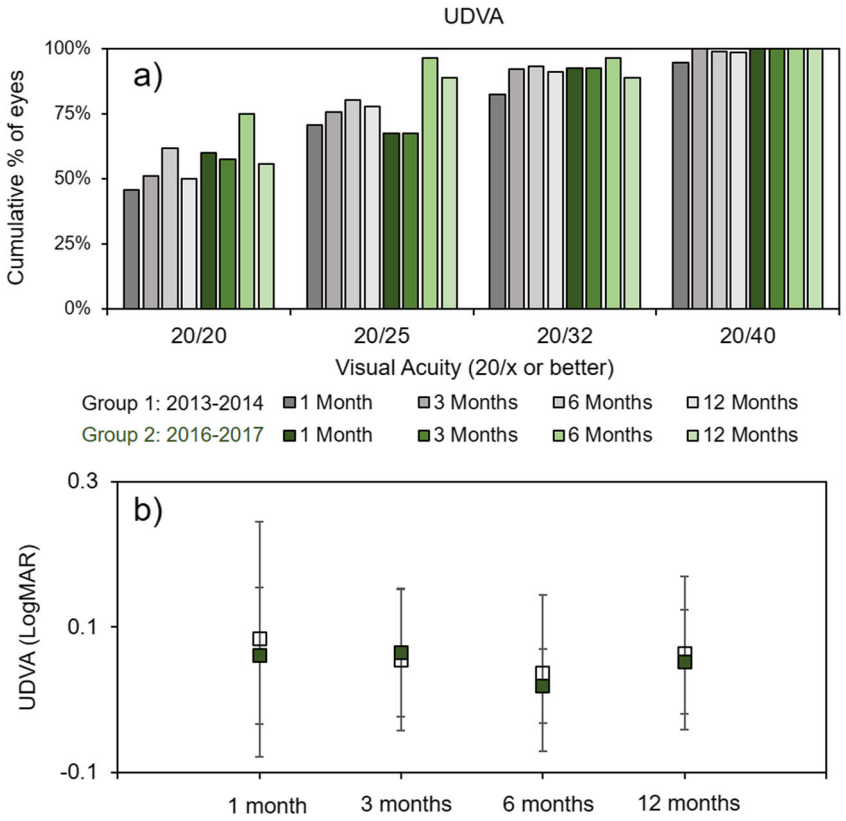

Fig. 11 **a** Outcomes in cumulative UDVA of group 1 (gray bars) and group 2 (green bars). **b** Progression in postoperative mean UDVA over 1 year

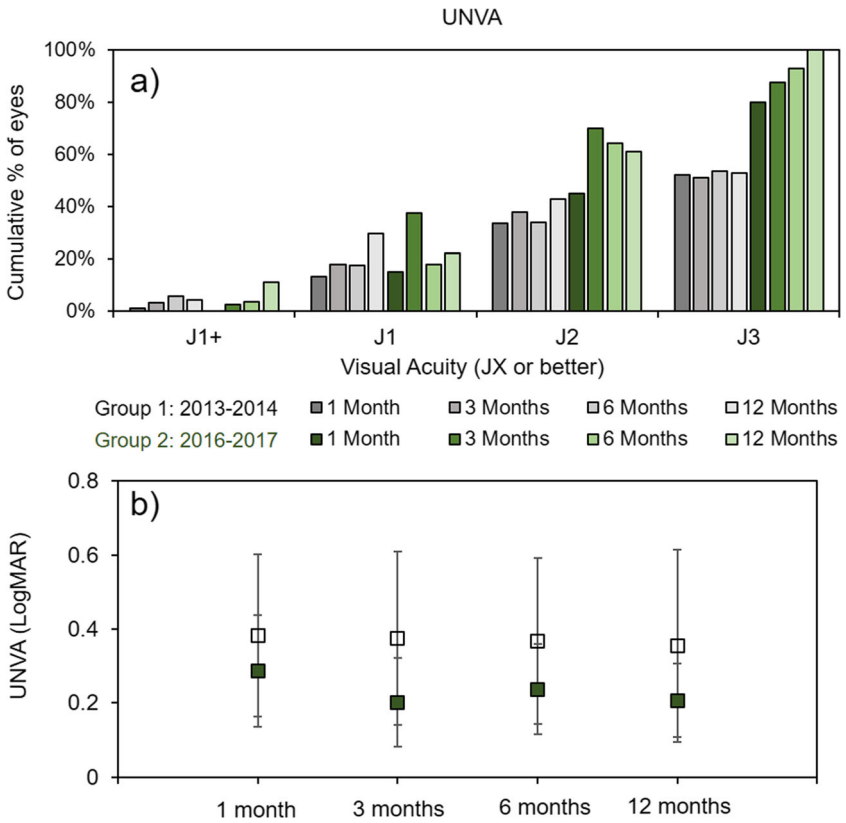

Fig. 12 **a** Cumulative distribution of UNVA; and b mean UNVA stated as LogMAR over the first year. Open and solid symbols in **b** represent the outcomes from group 1 and 2, respectively

the first year. The mean UNVA was 0.28 ± 0.28 (LogMAR) for group 1, while it was 0.20 ± 0.15 (LogMAR) for group 2. The mean UNVA at the first postoperative year for group 2 was found to be significantly better from the first postoperative month. Accordingly, the p values obtained from the Student's t test yielded 0.0141, 0.0441, 0.0001, and 0.0173 at 1, 3, 6, and 12 postoperative months, respectively.

Discussion

To review the benefits of improving corneal thickness in central symmetry and relocating the posterior corneal cone into the center, posterior corneal axial curvatures were analyzed in regard to the classified axial curvature maps according to Liu et al. (1999) [39]. However, the classified curvature maps were partly not suitable to match up with posterior axial curvature maps that were generated after peripheral presbyopia correction with asymmetric corneal ablation (PPA) correction. Thus, we copied or modified the patterns from the classified axial curvature maps, reclassified them into four distinct types, and converted the names to match the posterior axial curvature patterns generated by PPA correction. The patterns are divided into four types and classified as best (a) to worst (d) as depicted in Fig. 13. In group 1, the preoperative distribution of patients' posterior corneal axial curvature map patterns is 1.2% for a, 0% for b, 85.2% for c, and 13.6% for d. At the 12th postoperative month, the distribution changed to 35.1% for a, 21.6% for b, 32.4% for c, and 10.8% for d.

The results are in agreement with former results where, statistically, it could not be seen as a significant improvement in UNVA. The actual UNVA results were also analyzed as not having a significant improvement. In group 2, the preoperative distribution of patients' posterior axial curvature map patterns is 2% for a, 26% for b, 15% for c, and 57% for d. At the 12th postoperative month, the postoperative distribution of patients' posterior axial curvature map patterns changed to 57, 39, and 4% for a, b, and c, respectively and 0% for d. The central-symmetric corneal thickness and central posterior corneal cone dramatically reduced irregular curvature of posterior cornea. A series of results created in this study demonstrates the linkage that corneal curvature is influenced by corneal shape and corneal shape is influenced by intraocular pressure.

Initial LAK was applied to 84 eyes in group 1 during PPA correction. Advanced LAK was applied to 38 eyes in group 2 during PPA correction. Patients' SE in the two groups were approximately − 1D and were stable, postoperatively. However, there was a statistical improvement in central symmetry of cornea only in group 2. The main cause of the failure in group 1 is from using asymmetric corneal ablation patterns made by the 90° angled combination of semi-cylindrical ablation patterns, as depicted in Fig. 2b. This shape does not follow the basic principle that an asymmetric ablation pattern has to have a shape that progressively increases the ablation depth from the edge to the center, like the semi-cylindrical ablation pattern depicted in Fig. 2a. From this perspective, compare Fig. 2b with c. In Fig. 2b, the shape has two deepest ablation depths that are decentered. Thus, this shape is not suitable to correct normal corneal distortion caused by IOP. On the contrary, in Fig. 2c, the shape is made by the 45° angled combination of semi-cylindrical ablation patterns and it follows the basic principle. It has one deepest ablation depth at the center of the shape. Thus, it is suitable to use for correcting normal corneal distortion caused by intraocular

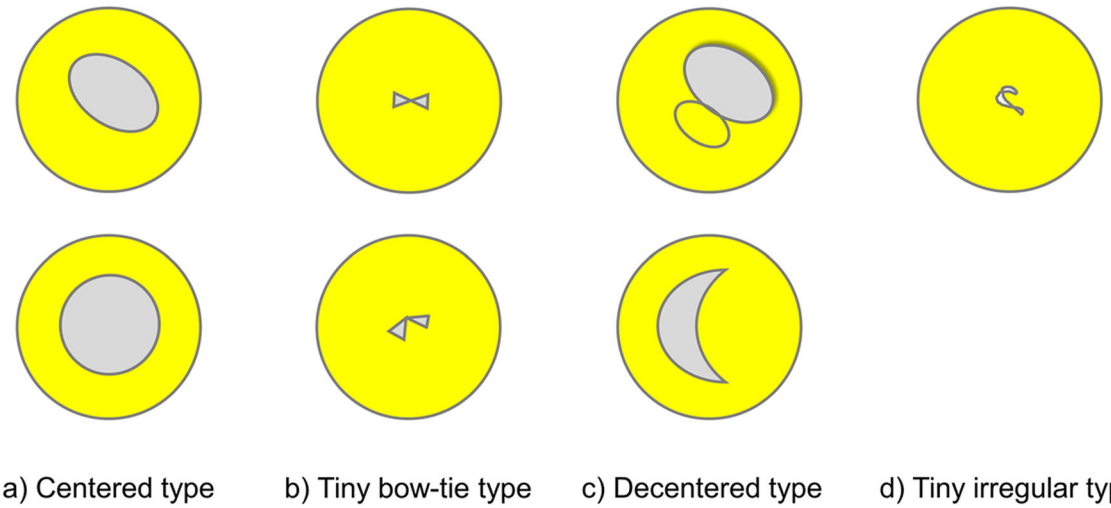

Fig. 13 Illustration of four types classification of posterior axial curvature map by PPA correction. The patterns were copied or modified from the axial corneal curvature maps classified by Liu et al. 1999

pressure. Here, normal corneal distortion means that the cornea has a single thickest point that is decentered.

The implementation of the self-developed image processing algorithm permits a systematic follow-up of the variation in corneal thickness and posterior corneal cone, and to figure out the position of the posterior corneal apex point relative to the visual axis. The corneal thickness variation factor, *f*, was improved only in patients who had the procedure performed between 2016 and 2017 (group 2). In group 2, the ablation procedure successfully achieved a significant improvement of corneal thickness in central symmetry and central posterior corneal cone was produced. As well, they also had a significant improvement in the alignment of the posterior corneal apex center with the visual axis.

The maps in Fig. 14 show a comparison of the postoperative maps in order to review the effects between PP correction, and peripheral presbyopia correction with asymmetric corneal ablation correction (PPA) used in Advanced LAK. Both corrections had the same target refraction: achieving SE of − 1D. The corneal map in Fig. 14a shows the anterior tangential curvature created by PP correction, central curvature secured for distance vision, and four partial arc-shaped myopic curvatures for near vision are placed outside the central 3-mm zone. The same method of PP correction as depicted in Fig. 14a was presented at the annual ARVO meeting in March 2012 [40]. The disadvantage of PP correction is near vision loss or vision discomfort at night or indoors in postoperative [40]. The corneal map in Fig. 14b shows the anterior tangential curvature at 2 postoperative year, central curvature for distance vision is secured in 5 mm circle, and ring-shaped myopic curvatures for near vision are placed outside the central 5 mm zone. Thus, it shows that PPA correction provides a more comfortable vision at night or indoors than PP correction.

Most contact lenses and intraocular lenses have a central-symmetric or a line-symmetric shape. It represents the basic optical concept that the shape of a symmetric lens decreases optical aberration than the shape of an asymmetric lens. The goal of LAK is to produce central-symmetric corneal thickness so that intraocular pressure helps in improving the asymmetric corneal shape to become symmetric. The maps in Fig. 15 show 4.3 postoperative year outcomes of the sample patient's cornea resulting from PPA correction used in Initial LAK. In the map of Fig. 15a, corneal thickness in the center and the periphery appears to be thicker than the map at 1 postoperative year, as depicted in Fig. 5a, mainly due to corneal edema. However, it does not have a problem in roughly checking the changes in its postoperative shape and curvature. Figure 15a, b demonstrates an increased central-symmetric thickness deviation and a decentered posterior cone after one postoperative year, but still better than its preoperative condition. Figure 15c shows a continued improvement of anterior axial curvature, postoperatively. We need to keep an eye on whether the changes in corneal shape due to regression will stop at this point, or it will stop after progressing a bit more. As well, the posterior tangential curvature maps in Figs. 6 and 15e show a continuously stable anterior tangential curvature for 4.3 postoperative years. In addition, the maps in Figs. 14b and 15e show that the ring-shaped myopic curvature created by Advanced LAK is clearer than the ring-shaped myopic curvature created by Initial LAK. The comparison of both maps explains why group 2 has better UCVA than group 1 postoperatively.

The disadvantage of LAK is that corneal curvature becomes asymmetric immediately after execution. Thus, our concern was that patients may experience vision discomfort immediately after surgery, due to the increase of curvature deviation. However, there were no complaints from patients regarding their postoperative vision. See the changes of the anterior axial corneal curvature in the maps of Figs. 5c and 15c. After executing LAK, anterior corneal curvature deviation in central symmetry immediately increased and then steadily decreased for 4.3 postoperative years.

The postoperative corneal maps shown above demonstrate that LAK contributes to reduce postoperative corneal distortion despite the fact that it was the first trial using the biomechanical approach to improve corneal shape. Our ultimate correction goal is to improve the corneal shape and maintain its shape at the best state. For a better outcome in future research, it will be necessary to improve the precision of ablation by LAK as well as an accurate analysis to quantify the time-dependent changes of each postoperative corneal shape and curvature.

In emmetropic or hyperopic presbyopia correction, the laser mainly ablates peripheral cornea. Then, peripheral corneal thickness becomes thinner and the thickness difference between the center and the periphery gets reduced. In this case, the success rate of posterior corneal cone relocating to the center is much less than when myopic presbyopia correction is performed. If the periphery becomes thinner than the central cornea after the surgery, the posterior corneal cone is positioned off center due to intraocular pressure and corneal distortion is generated. Myopic presbyopia correction helps intraocular pressure produce a central posterior corneal cone because the laser mainly ablates the corneal center. Thus, the clinical application according to the hypothesis is appropriate for myopic presbyopia correction.

In 2017, laser crescent keratectomy was suggested as a solution to treat keratoconus by reshaping the cornea after surgery [41]. The concept of crescent keratectomy is the same as LAK in terms of using intraocular pressure to reshape the cornea. Thus, laser crescent keratectomy can be one of the evidences that LAK can treat keratoconus by reducing the influence of intraocular pressure on thin regions of the cornea. In our opinion, LAK has the advantage of treating some of

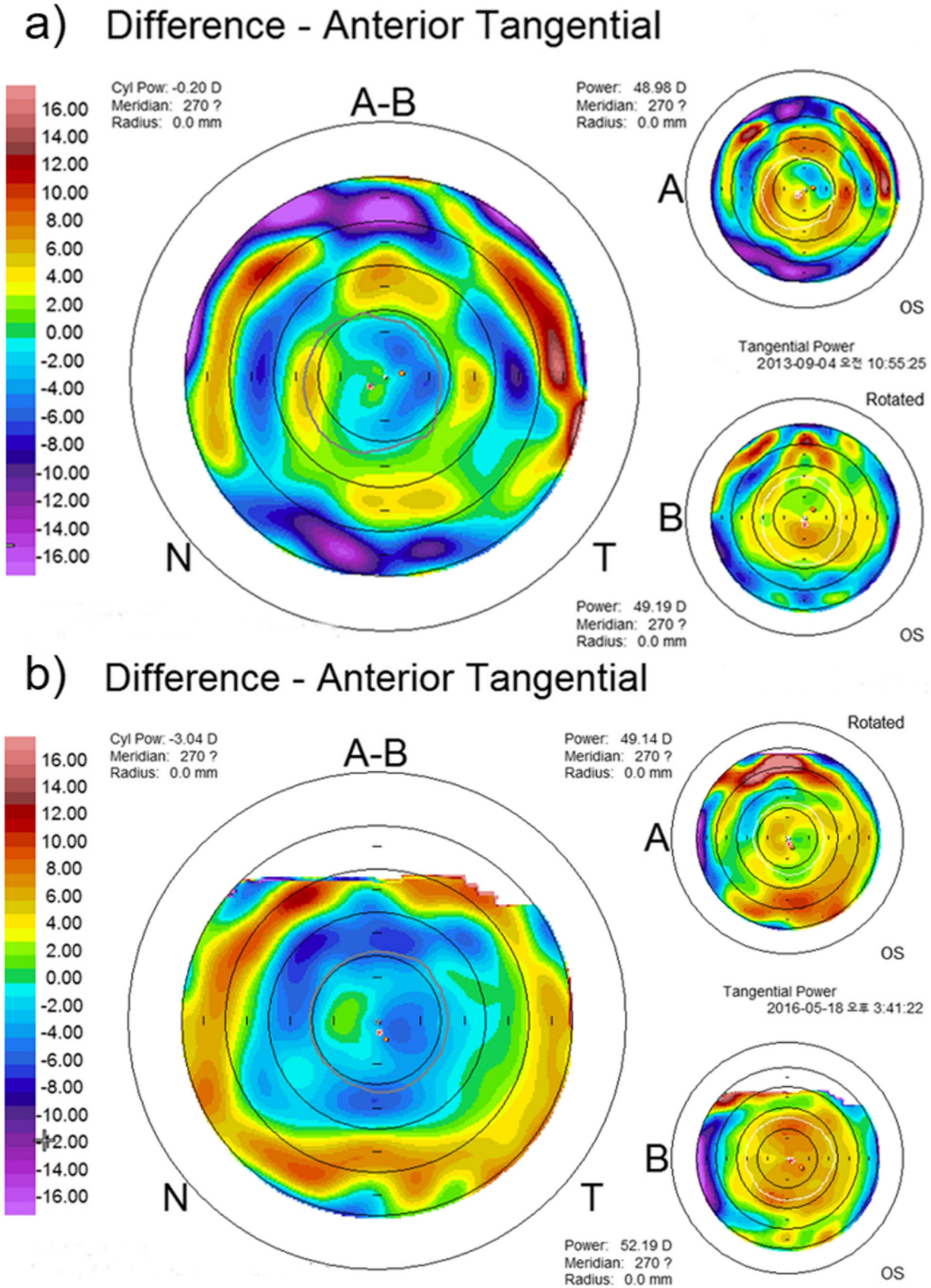

Fig. 14 Comparison of the postoperative maps between PP correction and PPA correction used in Advanced LAK

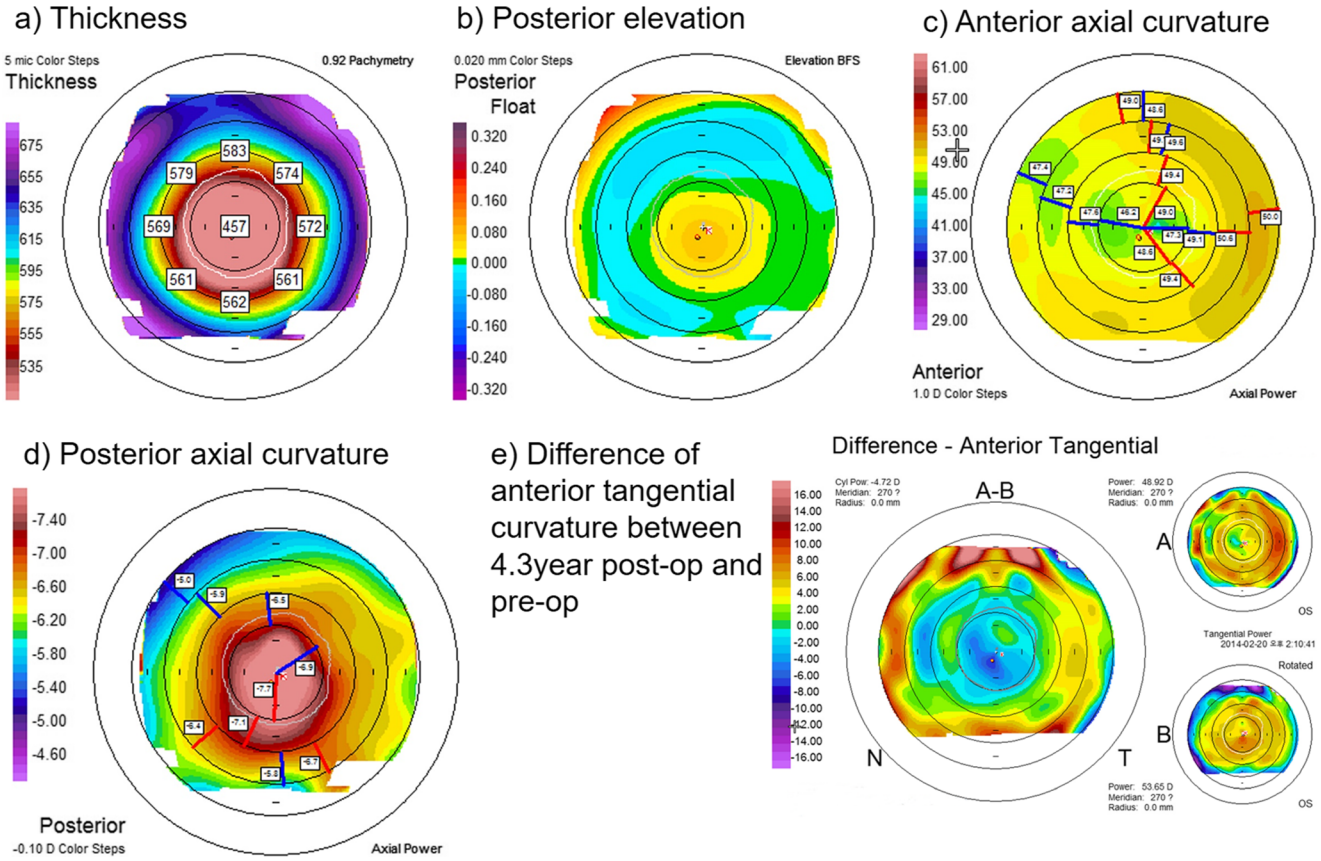

Fig. 15 The sample patient's 4.3-year postoperative maps

early and/or mild keratoconus. LAK has a simple operation process and can expect to produce the best corrected visual acuity through reducing corneal distortion compared to current methods. Therefore, we suggest the use of LAK for future researches in this field.

Funding information The authors received no specific funding for this work.

Compliance with ethical standards

Conflict of interest Kisung Park, Jinyoung Park, and Jina Park hold Europe, China, Japan, and US patents for the Laser Asymmetric Keratectomy (LAK) for point-symmetric corneal correction. None of the other authors has a financial or proprietary interest in any material or method mentioned.

Ethical approval All procedures performed in studies involving human participants were in accordance with the ethical standards of the institutional and/or national research committee and with the 1964 Helsinki declaration and its later amendments or comparable ethical standards. The National Bioethics Committee in Seoul, Republic of South Korea, stated that no IRB approval was required for the retrospective analysis of the data.

Informed consent Informed consent was obtained from all individual participants included in the study.

References

1. Sjontoft E, Edmund C (1987) In vivo determination of Young's modulus for the human cornea. Bull Math Biol 49(2):217–232
2. Elsheikh A, McMonnies CW, Whitford C, Boneham GC (2015) In vivo study of corneal responses to increased intraocular pressure loading. Eye Vision 2. https://doi.org/10.1186/s40662-015-0029-z
3. Polack FM (1961) Morphology of the cornea. I. Study with silver stains. Am J Ophthalmol 51:1051–1056
4. Komai Y, Ushiki T (1991) The three-dimensional organization of collagen fibrils in the human cornea and sclera. Invest Ophthalmol Vis Sci 32(8):2244–2258
5. Oyster CW (1999) The human eye: structure and function. Sinauer Associates Inc, Sunderland, MA
6. Hamada R, Giraud JP, Graf B, Pouliquen Y (1972) Analytical and statistical study of the lamellae, keratocytes and collagen fibrils of the central region of the normal human cornea. (Light and electron microscopy). Arch d'Ophtalmol Rev Gen d'Ophtalmol 32(8):563–570
7. Meek KM, Boote C (2004) The organization of collagen in the corneal stroma. Exp Eye Res 78(3):503–512
8. Newton RH, Meek KM (1998) Circumcorneal annulus of collagen fibrils in the human limbus. Invest Ophthalmol Vis Sci 39(7):1125–1134
9. Newton RH, Meek KM (1998) The integration of the corneal and limbal fibrils in the human eye. Biophys J 75(5):2508–2512. https://doi.org/10.1016/s0006-3495(98)77695-7
10. Boote C, Dennis S, Huang Y, Quantock AJ, Meek KM (2005) Lamellar orientation in human cornea in relation to mechanical properties. J Struct Biol 149(1):1–6. https://doi.org/10.1016/j.jsb.2004.08.009

11. Meek KM (2008) The cornea and sclera. In: Fratzl P (ed) Collagen, structure and biomechanics. Springer Science, New York
12. Schmack I, Dawson DG, McCarey BE, Waring GO 3rd, Grossniklaus HE, Edelhauser HF (2005) Cohesive tensile strength of human LASIK wounds with histologic, ultrastructural, and clinical correlations. J Refract Surg 21(5):433–445
13. Dawson DG, Kramer TR, Grossniklaus HE, Waring GO 3rd, Edelhauser HF (2005) Histologic, ultrastructural, and immunofluorescent evaluation of human laser-assisted in situ keratomileusis corneal wounds. Arch Ophthalmol 123(6):741–756. https://doi.org/10.1001/archopht.123.6.741
14. Smadja D, Santhiago MR, Mello GR, Roberts CJ, Dupps WJ Jr, Krueger RR (2012) Response of the posterior corneal surface to myopic laser in situ keratomileusis with different ablation depths. J Cataract Refract Surg 38(7):1222–1231. https://doi.org/10.1016/j.jcrs.2012.02.044
15. Muller L, Pels E, Vrensen G (2001) The specific architecture of the anterior stroma accounts for maintenance of corneal curvature. Br J Ophthalmol 85(4):437–443. https://doi.org/10.1136/bjo.85.4.437
16. Hamilton DR, Johnson RD, Lee N, Bourla N (2008) Differences in the corneal biomechanical effects of surface ablation compared with laser in situ keratomileusis using a microkeratome or femtosecond laser. J Cataract Refract Surg 34(12):2049–2056. https://doi.org/10.1016/j.jcrs.2008.08.021
17. Qazi MA, Sanderson JP, Mahmoud AM, Yoon EY, Roberts CJ, Pepose JS (2009) Postoperative changes in intraocular pressure and corneal biomechanical metrics laser in situ keratomileusis versus laser-assisted subepithelial keratectomy. J Cataract Refract Surg 35(10):1774–1788. https://doi.org/10.1016/j.jcrs.2009.05.041
18. Sutton GL, Kim P (2010) Laser in situ keratomileusis in 2010—a review. Clin Exp Ophthalmol 38(2):192–210. https://doi.org/10.1111/j.1442-9071.2010.02227.x
19. Ortiz D, Pinero D, Shabayek MH, Arnalich-Montiel F, Alio JL (2007) Corneal biomechanical properties in normal, post-laser in situ keratomileusis, and keratoconic eyes. J Cataract Refract Surg 33(8):1371–1375. https://doi.org/10.1016/j.jcrs.2007.04.021
20. Ambrósio R, Wilson SE (2003) LASIK vs LASEK vs PRK: advantages and indications. Semin Ophthalmol 18(1):2–10. https://doi.org/10.1076/soph.18.1.2.14074
21. Roberts C (2000) The cornea is not a piece of plastic. J Refract Surg 16(4):407–413
22. Hernández-Quintela E, Samapunphong S, Khan BF, Gonzalez B, Lu PC-S, Farah SG, Azar DT (2001) Posterior corneal surface changes after refractive surgery. Ophthalmology 108(8):1415–1422
23. Wang Z, Chen J, Yang B (1999) Posterior corneal surface topographic changes after laser in situ keratomileusis are related to residual corneal bed thickness. Ophthalmology 106(2):406–410
24. Kamiya K, Oshika T, Amano S, Takahashi T, Tokunaga T, Miyata K (2000) Influence of excimer laser photorefractive keratectomy on the posterior corneal surface. J Cataract Refract Surg 26(6):867–871
25. Miyata K, Kamiya K, Takahashi T, Tanabe T, Tokunaga T, Amano S, Oshika T (2002) Time course of changes in corneal forward shift after excimer laser photorefractive keratectomy. Arch Ophthalmol 120(7):896–900
26. Kim H, Kim HJ, Joo C-K (2006) Comparison of forward shift of posterior corneal surface after operation between LASIK and LASEK. Ophthalmologica 220(1):37–42
27. Ciolino JB, Belin MW (2006) Changes in the posterior cornea after laser in situ keratomileusis and photorefractive keratectomy. J Cataract Refract Surg 32(9):1426–1431. https://doi.org/10.1016/j.jcrs.2006.03.037
28. Ciolino JB, Khachikian SS, Cortese MJ, Belin MW (2007) Long-term stability of the posterior cornea after laser in situ keratomileusis. J Cataract Refract Surg 33(8):1366–1370. https://doi.org/10.1016/j.jcrs.2007.04.016
29. Vicente D, Clinch TE, Kang PC (2008) Changes in posterior corneal elevation after laser in situ keratomileusis enhancement. J Cataract Refract Surg 34(5):785–788. https://doi.org/10.1016/j.jcrs.2007.12.040
30. Chan TCY, Biswas S, Yu M, Jhanji V (2015) Longitudinal evaluation of cornea with swept-source optical coherence tomography and Scheimpflug imaging before and after Lasik. Medicine 94(30). https://doi.org/10.1097/md.0000000000001219
31. Seiler T, Koufala K, Richter G (1998) Iatrogenic keratectasia after laser in situ keratomileusis. J Refract Surg 14(3):312–317
32. Seiler T, Quurke AW (1998) Iatrogenic keratectasia after LASIK in a case of forme fruste keratoconus. J Cataract Refract Surg 24(7):1007–1009
33. Lee MJ, Lee SM, Lee HJ, Wee WR, Lee JH, Kim MK (2007) The changes of posterior corneal surface and high-order aberrations after refractive surgery in moderate myopia. Korean J Ophthalmol 21(3):131–136. https://doi.org/10.3341/kjo.2007.21.3.131
34. Oshika T, Klyce SD, Applegate RA, Howland HC, El Danasoury MA (1999) Comparison of corneal wavefront aberrations after photorefractive keratectomy and laser in situ keratomileusis. Am J Ophthalmol 127(1):1–7
35. Seiler T, Kaemmerer M, Mierdel P, Krinke HE (2000) Ocular optical aberrations after photorefractive keratectomy for myopia and myopic astigmatism. Arch Ophthalmol 118(1):17–21
36. Chalita MR, Chavala S, Xu M, Krueger RR (2004) Wavefront analysis in post-LASIK eyes and its correlation with visual symptoms, refraction, and topography. Ophthalmology 111(3):447–453. https://doi.org/10.1016/j.ophtha.2003.06.022
37. Sharma M, Wachler BS, Chan CC (2007) Higher order aberrations and relative risk of symptoms after LASIK. J Refract Surg 23(3):252–256
38. Kirwan C, O'Keefe M (2009) Comparative study of higher-order aberrations after conventional laser in situ keratomileusis and laser epithelial keratomileusis for myopia using the technolas 217z laser platform. Am J Ophthalmol 147(1):77–83. https://doi.org/10.1016/j.ajo.2008.07.014
39. Liu Z, Huang A, Pflugfelder S (1999) Evaluation of corneal thickness and topography in normal eyes using the Orbscan corneal topography system. Br J Ophthalmol 83(7):774–778
40. Park WC, Rho SH, Jin SW, Park KS, Min BM, Lee JH (2012) The long-term result of corneal correction of presbyopia with Kera laser. Invest Ophthalmol Vis Sci 53(14):289–289
41. Carriazo C, Cosentino M (2017) A novel corneal remodeling technique for the management of keratoconus. J Refract Surg 33:854–856. https://doi.org/10.3928/1081597X-20171004-05